

Evaluation of Petro Physical Properties of the Reservoirs in XY Field Gulf of Mexico (GOM)

Oko, Christian Obinna¹, Igbo, Nkechinyere Elem², Igbo, Michael Elem^{3*}, and Kalu, Jonah⁴.
^{1,2,3,4}Department of Science Laboratory Technology, Federal Polytechnic Afikpo, Ebonyi State, Nigeria.

Abstract:- A composite log suite that comprised of gamma ray, resistivity, density and neutron logs of six wells (Agate, Diamond, Apatite, Calcite, Copper and Jasper) were employed to evaluate the petrophysical properties of the reservoirs of interest in XY field Gulf of Mexico. This was done to evaluate the trend and values of the petrophysical properties of the reservoirs in the field, while the objective was to delineate and predict the reservoir system quality and performance.

Correlation was carried out across the 6 wells using gamma ray, resistivity, neutron and density logs. The distribution and occurrence of these lithostratigraphic units appeared to reflect the influence of basin morphology and sea level variation. Tops and bases of 6 reservoirs of interest were mapped. Shale Volumes (Vsh) were computed using gamma ray log; the reservoir versus non-reservoir was delineated by applying cut-off of 80% computed volume of shale with the guide of spontaneous potential (SP) and deep resistivity logs for wells Agate and Diamond.

Computed Vsh was used for effective porosity to discount for the effects of clay bound water. The average porosity values ranged from 15 – 35% and 10 – 30%, Permeability averages of about 43mD – 75mD and 45mD – 118mD, and water saturation values averaging from 14.7% - 76.6% and 13.8% - 82% were gotten across the reservoirs in wells Agate and Diamond respectively.

Keywords:- Basin Morphology, Gulf of Mexico, Permeability, Porosity, Reservoir Sand, Shale Volume, Water Saturation, Well Logs.

I. INTRODUCTION

The study area, XY field Gulf of Mexico, is an ocean basin that lies between North American plate and the Yucatan block. Its depocenter consists of sediments that have been deposited in time from the Jurassic period through to the Holocene period with thickness of about 20km [3]. Sediments from the North American continent filled almost half of the basin, primarily by offlap of the northern margin and northwestern margin. The basin currently has an abyssal plain that lies at a depth of 3km [4].

In the east, the Gulf floor is dominated by morphology akin to the Late Quaternary Mississippi fan while the northern Gulf margin shows a bathymetrically complex morphology that terminated abruptly in the Sigsbee escarpment in the west and merged into the Mississippi fan in the east [14]. In the west, the Gulf margin shows intermediate width that is bathymetrically complex. In recent times, the shelf edge reflects a well-defined increase in basinward gradient lying generally at a depth of about 100–120 m. The northern, eastern and northwestern Gulf of Mexico is bounded by broad and low-gradient shelves with thickness that range from 100 to 300 km in the landward direction. Presently, the Florida and Yucatan platforms, which bound the Gulf basin on the east and south, persist as sites of carbonate deposition.

Onshore, the north and northwest Gulf margin shows broad coastal plain. At the lower coastal plain, Neogene and Quaternary strata underlies the flat and low-relief surface plain while the upper plain shows a modest relief that is less than 100m created by the incision of Quaternary strata into older Neogene, Paleogene, and Late Cretaceous strata through numerous small and large rivers. Various sediments from Cenozoic, Mesozoic, and remnant Paleozoic uplands which includes, the Lower Cretaceous limestone-capped Edwards Plateau, the Sierra Madre Oriental of Mexico, Ouachita Mountains of southern Arkansas, the Trans-Pecos mountains of West Texas, and the Cumberland Plateau and southern Appalachian Mountains of northern Mississippi and Alabama, bounds the Gulf basin [5].

The northeastern Gulf basin merged into the south Atlantic coastal plain across northern Florida with the structural basin boundary generally placed very close to the current west coast of the Florida peninsula [8].

II. MATERIALS

Materials used for this research work includes PETREL software, TECHLOG software, ECLIPSE software and other research and training materials.

2.1. DATA INVENTORY

Summary of dataset used for the purpose of this research work is presented on table shown below;

Input Data Set Requirement for Geological/Geophysica/Petrophysical Evaluation Studies																
Data Set Type	Welllogs															
NAMEWELL	CHECKSHOT	CALI	CILD	DPHI	DRHO	DT	GR	ILD	ILM	NPHI	PHIT	RHOB	RT	SFLU	SP	VCL
AGATE	YES	YES	YES	YES	YES	YES	YES	YES	YES	YES	YES	YES	YES	YES	YES	YES
APATITE	YES	NO	YES	YES	NO	YES	YES	YES	NO	YES	YES	NO	YES	YES	YES	YES
CALCITE	YES	NO	YES	NO	NO	YES	YES	YES	YES	NO	YES	NO	YES	YES	YES	YES
COPPER	YES	YES	YES	NO	YES	YES	YES	YES	NO	NO	YES	YES	YES	NO	YES	YES
DIAMOND	YES	YES	YES	YES	YES	YES	YES	YES	YES	YES	YES	YES	YES	YES	YES	YES
JASPER	YES	NO	YES	NO	NO	YES	YES	YES	NO	NO	YES	NO	YES	NO	YES	YES
	Seismic	YES														
	PVT	NO														
	Tops	YES														
	Well test	NO														
	Core Logs	NO														
	Capillary Pressure Data	NO														

Table 1. Data Inventory Table for the six wells of interest

➤ WELL LOG DATA

All the wells had caliper (CILD), Sonic (DT), Gamma Ray (GR), resistivity (ILD), porosity (PHIT), spontaneous potential (SP), and clay volume (VCL). Four wells had fluid saturation (SFLU) and three wells had caliper (CAL), density porosity (DPHI), density (RHOB), density correction (DRHO), resistivity (ILM), neutron (NPHI).

➤ GEOLOGICAL SETTING

Gulf of Mexico Basin is ranked among the world’s great petroleum mega-provinces, with hydrocarbon production history of more than 100 years. It is a rift basin located between North America and the Yucatan Block. The field is adjacent to the Caribbean Sea and surrounded by Eastern Mexico, Texas, the Southeastern Gulf States of the United States, and Cuba.

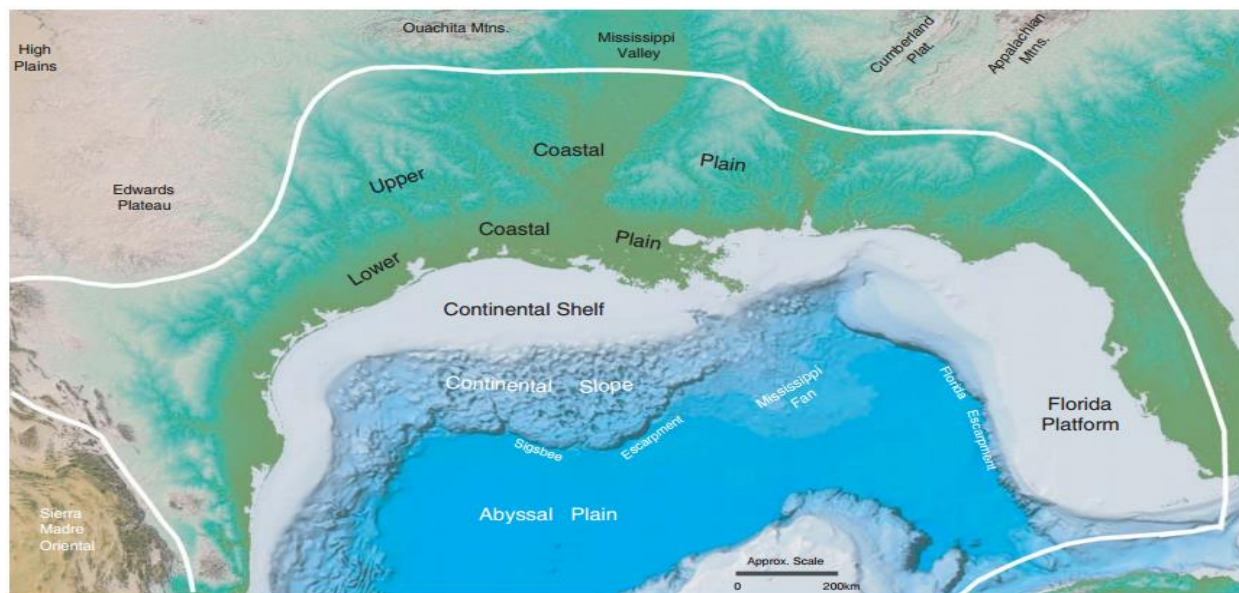


Figure 1. Physiographic elements of the Gulf basin, showing adjacent North America. The white outline shows approximate geological limits of the basin.

➤ WELL LOCATION

The six wells of interest are located on the Texas-Louisiana shelf. The shelf has a thickness of about 100km off the Rio Grande in Texas and more than 200km in the southern part of Texas-Louisiana boundary. Large amounts

of salt sedimentary sequence in the northwestern part of the Gulf shelf is the prominent structural feature in the area. The imminent effect of the salt in the area is the high tectonic movement of the shelf caused principally by the salt depositional sequence.

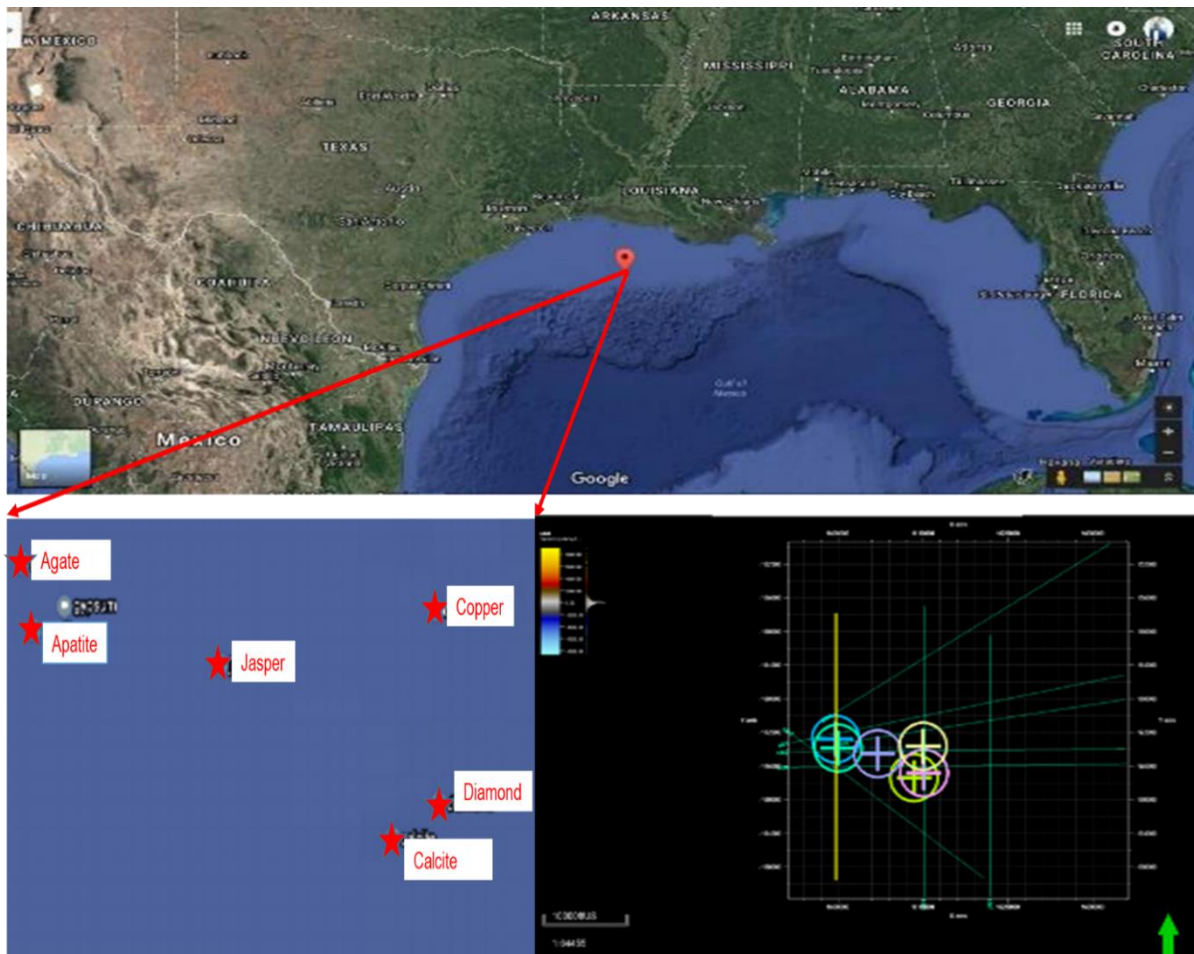


Figure 2. (a) Showing the wells location in the GoM (b) Showing enlarged view of the wells in the study location. (c) Showing wells location on a 2D Petrel window

III. METHOD

An integrated approach was applied in this study. The knowledge from the various subsurface disciplines was employed to develop 3D Reservoir Model of the field with the help of Schlumberger Oilfield Services Software (PETREL, TECHLOG AND ECLIPSE) in Portharcourt. Interdisciplinary reviews and interpretations were provided at each milestone of this project to ensure consistency in the geological, geophysical and reservoir engineering concepts of the study.

The processes employed in the study include:

- Data load, QA/QC, and data conditioning
- Sonic log calibration (TDR generation)
- Synthetic generation
- Well-to-seismic tie
- Seismic interpretation (fault and horizon interpretation)
- Generating surfaces for the reservoirs of interest
- Velocity modeling
- Time to Depth conversion
- Structural modeling of faults and horizons
- 3D grid model building (static), zoning and layering of the grids
- Property modeling
- Data analysis

3.1. STRUCTURAL MODELING

A structural model is regarded as the skeleton or container of the subsurface. It is the geological model of the area otherwise called the Geomodel [7]. To model any geologic subsurface, the modeler starts with a sound structural framework of the area which represents the relation between the faults and the seismic horizons showing the important layers of interest [12]. Structural modeling in Petrel involves Pillar Gridding, Fault Modeling, and Horizon picking (Layering).

Fault Modeling: The first step in fault modeling with petrel involves defining the faults of interest [1]. This helps to define the shape of each fault that must be modeled. The process was achieved by generating “Key Pillars”.

Pillar Gridding: Pillar gridding involves making grids based on the already defined faults. In this stage, a set of pillars was inserted in between interpreted faults and in every corner of the grids in the entire project area. The result of this process is a “Skeleton grid”, defined by all the faults and all the pillars.

Layering: After the fault modeling and the pillar gridding process, horizons were inserted into the faulted 3D grid. The 3D grid was converted to time/depth by associating it with time/depth maps and well tops. After inserting the horizons,

the zones of interest (based on geological input such as isochors) were inserted, and the final step was to make fine-

scale layerings suitable for property modeling.

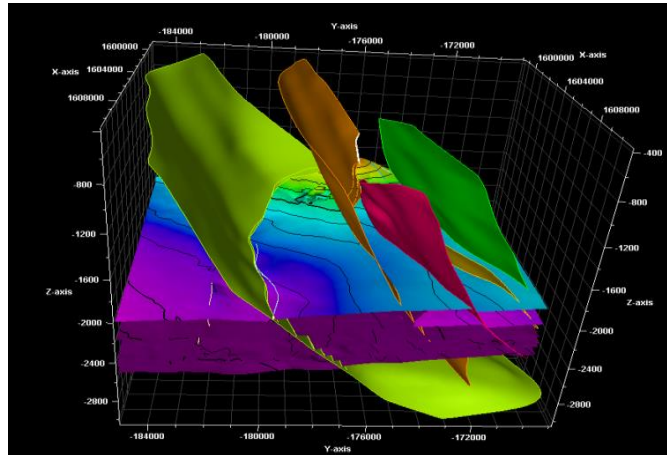


Figure 3. Fault and Horizon structural frameworks

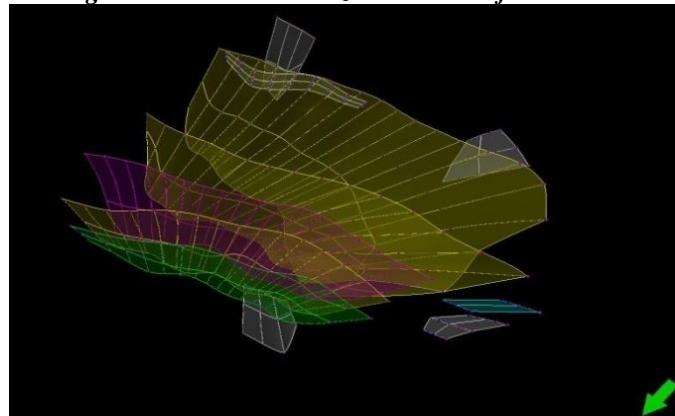


Figure 4. Pillar grid fault framework

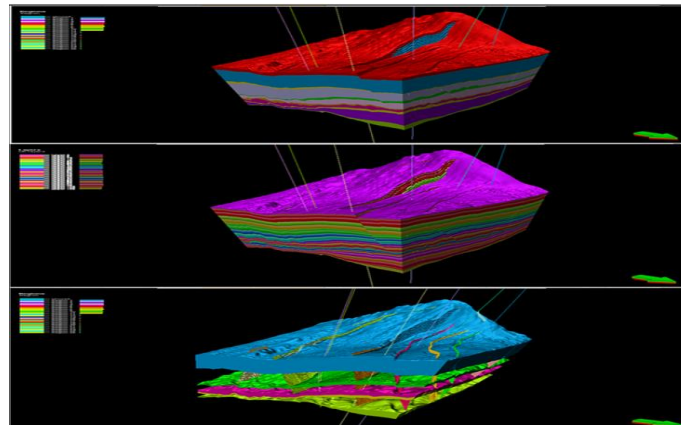


Figure 5. Layered structural model

➤ *Property Modeling*

Property modeling involves filling the 3D grid cells with discrete/continuous properties. The goal is to achieve a realistic property model by using all geological information available to build the model [13]. The Property modeling of the field was done with Petrel software and the process was split into three steps:

Geometrical modeling: This involves using some pre-defined functions to generate properties such as Bulk Volume, Depth, Height above Contact, and more [2]. These

properties are very important in volumetric evaluations and in mathematical operations between petrophysical properties (e.g. for Sw transforms).

Facies modeling: This involved the population of discrete data such as lithofacies, into 3D grid cells. This helps to give true understanding of the geological processes, and to capture facies architectures like reservoir connectivity, high level of heterogeneity and to confirm descriptive facies information such as shape, size, orientation, proportion, distribution and statistics.

Petrophysical modeling: This involves the interpolation and simulation of continuous data such as porosity, permeability and saturation into the 3D grid cells [9]. The petrophysical properties vary from facies to facies i.e.

different petrophysical property distributions in different facies with spatial variations for each petrophysical parameter.

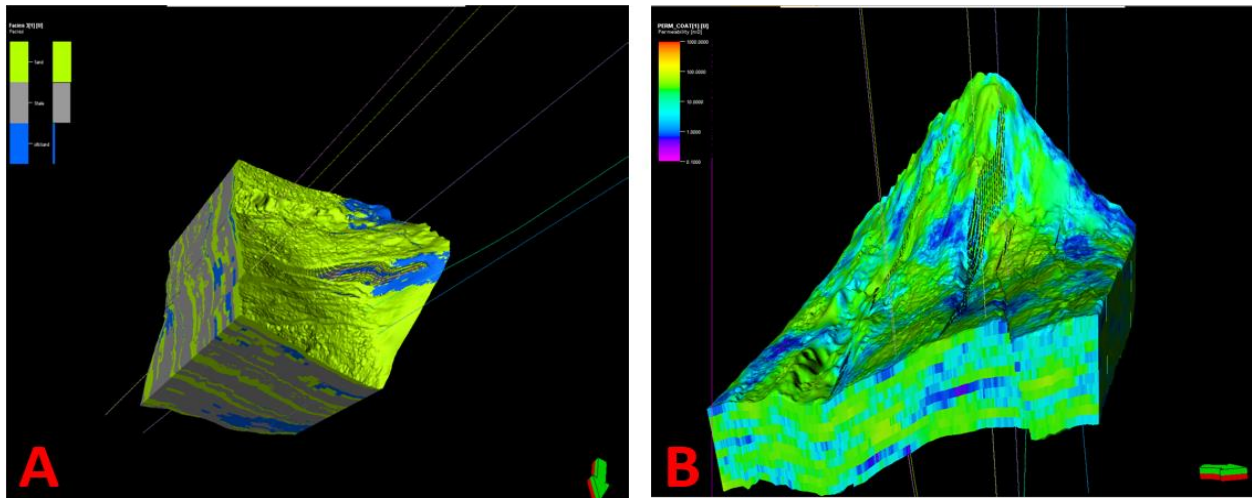


Figure 6. 3D Grid showing (A) facies distribution and (B) Porosity distribution

➤ *Model Upscaling*

Model upscaling involves merging the fine cells of the 3D Grid to obtain a coarse model while still preserving the geologic features important to the reservoir flow dynamic. For this study a 4:1 flow-based upscale was performed to

retain important flow characteristics of the fine-scale model. This was done to generate a stable and fast simulation model which is important and critical to allow the engineers spend enough time interpreting results and testing more scenarios.

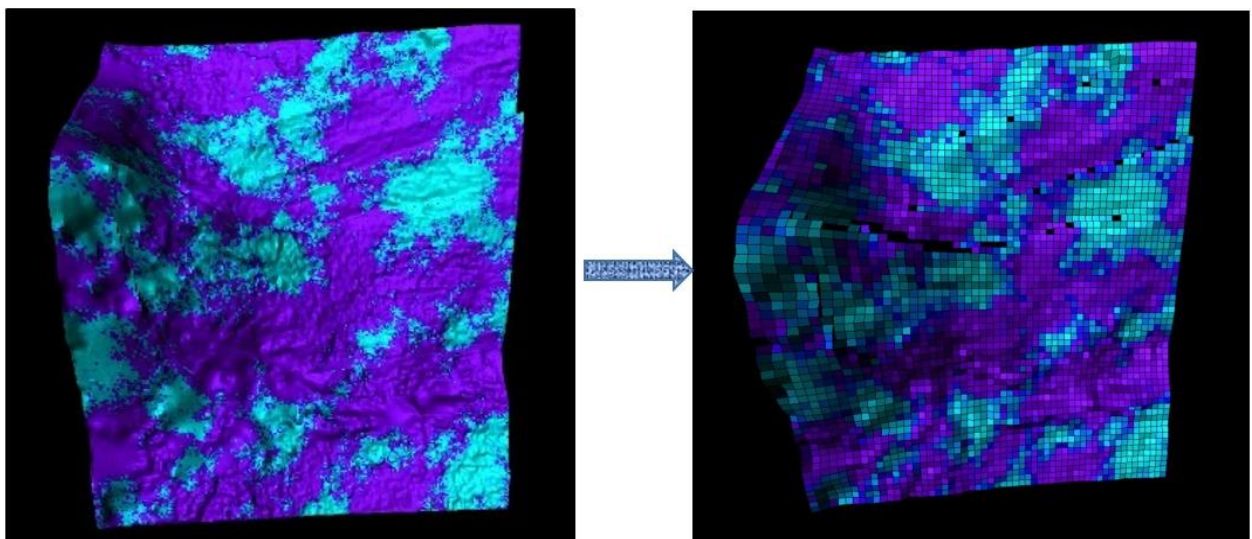


Figure 7. Showing fine scale and coarse scale 3D grid geomodel

IV. RESULTS AND DISSCUSSIONS

4.1. Petrophysical Evaluation

Petrophysical evaluation carried out on the measured log using the resistivity (ILD), gamma ray (GR), and crossplot of neutron (NPHI) and density (RHOB) logs indicated the presence of hydrocarbon within intervals of high resistivity and neutron density crossovers. This is the case in the two control wells, Agate and Diamond wells as

can be seen in figure 8, below. Due to lack of neutron and density logs on wells Apatite, Calcite, Copper and Jasper, conclusions could not be made on the presence of hydrocarbons on the different reservoir intervals.

Average porosity across the reservoirs is 0.30 - 0.40. Kobe reservoir contains gas while the other reservoir contains oil.

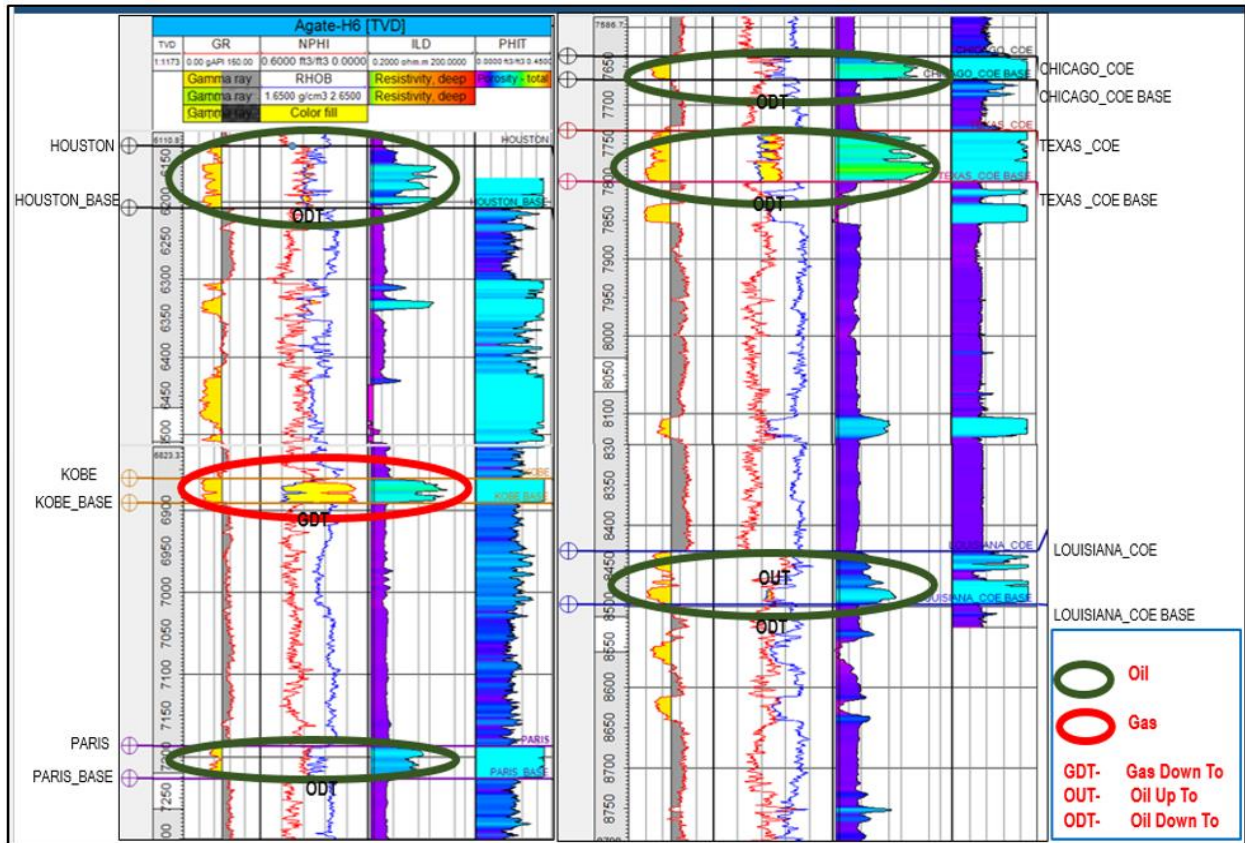


Figure 8. Result showing reservoirs of interest and hydrocarbon type throughout the column of well Agate

4.2. Petrophysical Properties

Shale Volumes (Vsh) were computed using gamma ray log; the reservoir versus non-reservoir was delineated by applying cut-off of 80% computed volume of shale with the guide of spontaneous potential (SP) and deep resistivity logs for wells Agate and Diamond. Computed Vsh was used to effective porosity to discount for the effects of clay bound

water. The average porosity values ranged from 15 – 35% and 10 – 30%, Permeability averages of about 43mD – 75mD and 45mD – 118mD, and water saturation values averaging from 14.7% - 76.6% and 13.8% - 82% were gotten across the reservoirs in wells Agate and Diamond respectively.

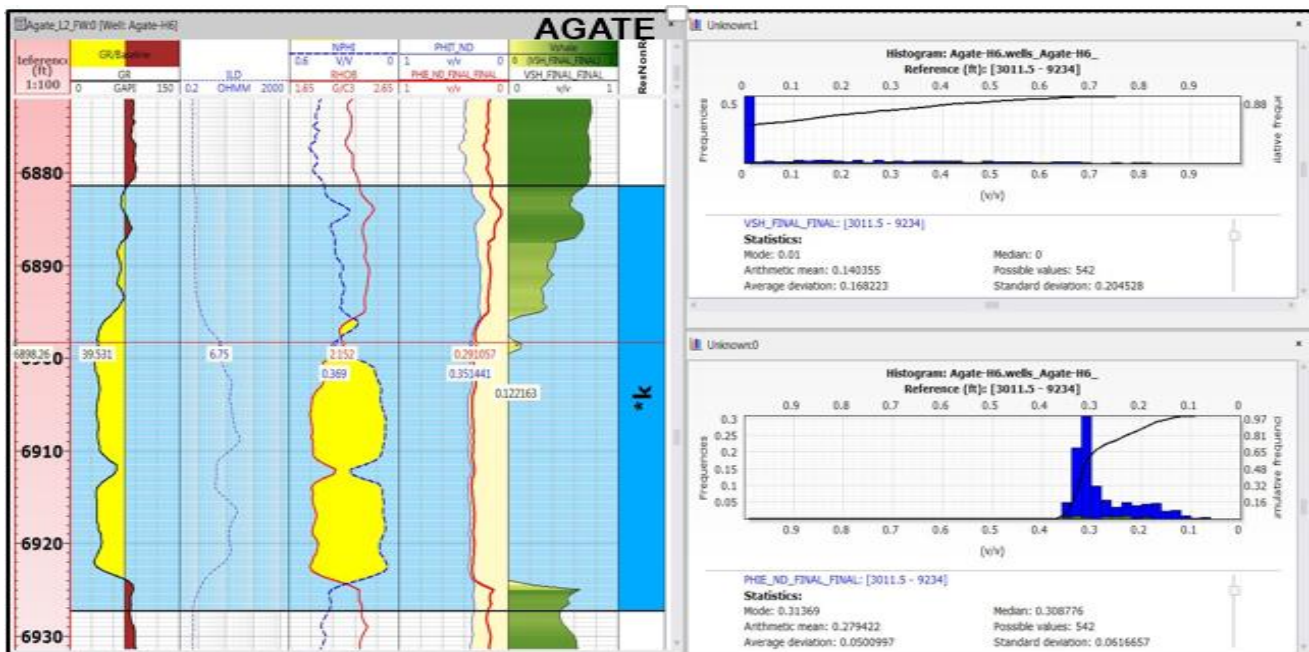


Figure 9. Result of the shale volume and effective porosity curves generated for well Agate

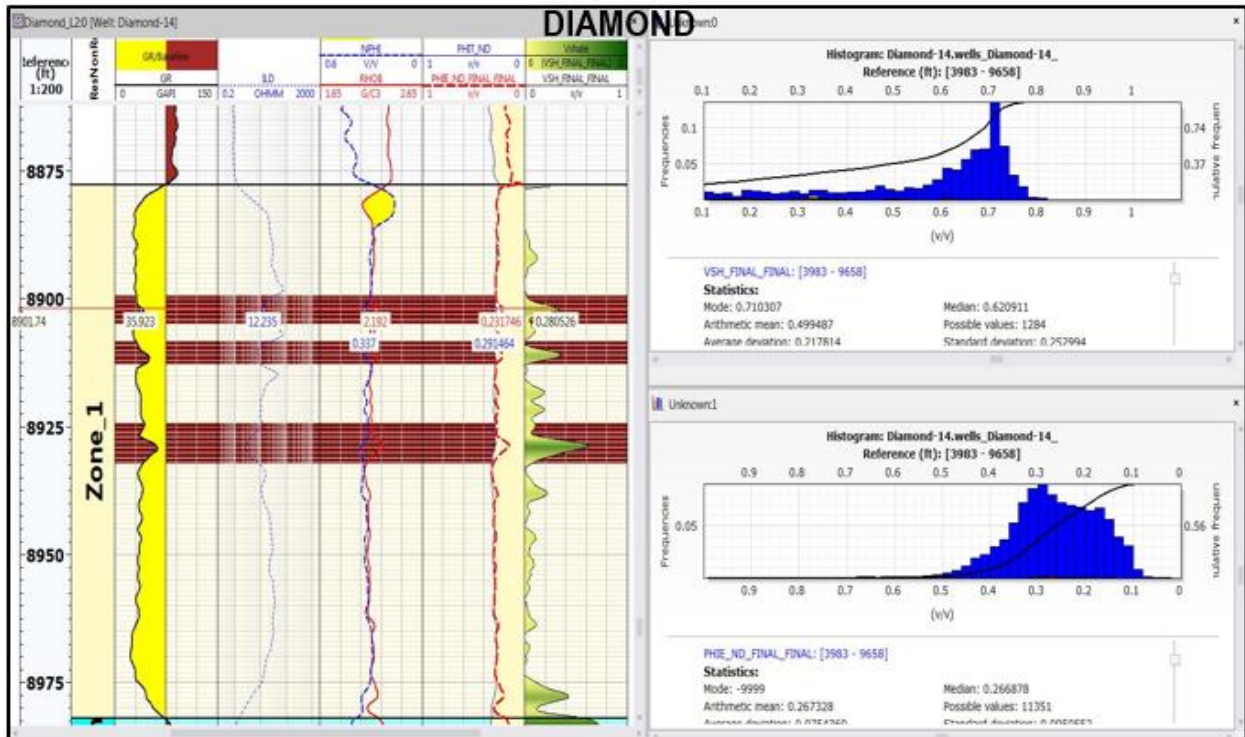


Figure 10. Result of the shale volume and effective porosity curves generated for well Diamond

	Well	Top	Bottom	Reference unit	Gross	Net	Net to Gross	Av_Shale Volume	Av_Porosity	Av_Water Saturation
1	Agate-H6	6089.025	6183.049	ft	94.023	2.5	0.027	0.261	0.374	0.806
2	Agate-H6	6183.049	6241.637	ft	58.588	49	0.836	0.276	0.366	0.427
3	Agate-H6	6338.333	6378.569	ft	40.235	16.5	0.41	0.245	0.358	0.484
4	Agate-H6	6458.813	6542.802	ft	83.989	3.5	0.042	0.27	0.347	0.819
5	Agate-H6	6542.802	6893.528	ft	350.726	13	0.037	0.272	0.356	0.655
6	Agate-H6	6893.528	6925.467	ft	31.938	30.472	0.954	0.231	0.343	0.384
7	Agate-H6	6893.528	6925.467	ft	31.938	27.5	0.861	0.199	0.351	0.333
8	Agate-H6	7220.541	7265.4	ft	44.859	37.5	0.836	0.317	0.343	0.528
9	Agate-H6	7684.871	7721.7	ft	36.829	31.2	0.847	0.345	0.321	0.392
10	Agate-H6	7721.7	7785.095	ft	63.395	0.3	0.005	0.714	0.275	0.791
11	Agate-H6	7785.095	7918.106	ft	133.012	68	0.511	0.276	0.349	0.267
12	Agate-H6	8184.33	8214.244	ft	29.914	27.5	0.919	0.321	0.337	0.48
13	Agate-H6	8528.502	8754.707	ft	226.205	34.5	0.153	0.211	0.324	0.556
14	Diamond-14	8876.618	8983.662	ft	107.044	104.382	0.975	0.267	0.293	0.357
15	Diamond-14	8876.618	8983.662	ft	107.044	101	0.944	0.254	0.294	0.338
16	Diamond-14	9233.857	9300.98	ft	67.123	65.623	0.978	0.488	0.309	0.88
17	Diamond-14	9233.857	9300.98	ft	67.123	22	0.328	0.356	0.315	0.658
18	Diamond-14	9456.169	9575.418	ft	119.249	83.331	0.699	0.538	0.282	0.766
19	Diamond-14	9456.169	9575.418	ft	119.249	38.5	0.323	0.403	0.294	0.53

Table 2. Petrophysical evaluation table (reservoir sums and averages for wells Agate and Diamond)

V. CONCLUSION

In conclusion, this research work evaluated the petrophysical properties of the reservoir sand bodies of XY field Gulf of Mexico (GOM). Six wells of interest were picked for this study. Existing seismic, together with available well logs were interpreted. Thus, the Horizons (layer tops) representing the six reservoirs of interest were picked while faults were interpreted to define the storage container boundaries. Structural and petrophysical analysis of the field was done and the results from the study shows that the average porosity values of the field ranged from 15% - 35% and 10% - 30% in wells Agate and Diamond Permeability values of 43mD – 75mD and 45mD – 118mD, and water saturation values averaging from 14.7% - 76.6% and 13.8% - 82% were gotten across the reservoirs in wells Agate and Diamond respectively.

Due to lack of neutron and density logs on wells Apatite, Calcite, Copper and Jasper, conclusion could not be made on the petrophysical properties of the wells on the different reservoirs intervals.

REFERENCES

- [1]. Adeeba, R. S., (2009). Reservoir Modeling with Petrel and Simulation run with FrontSim, presented to Department of petroleum and Mining, Chittagong University of Engineering and Technology. Chittagong, Bangladesh.
- [2]. Ajeet, K. P., Ravendra, K., Manish, S., Anil, N., Tandon, A. K., (2013). Seismic Velocity Model Buildin: An aid for better understanding of subsurface- A case study from Cambay Basin, India. SPG 10th Biennial International Conference and Exposition, P408.
- [3]. Ananev, V. V., Verzhbitskiy, V. E., Obukhov, A. N., Borisov, D. V., Nortsev, G. V., (2014). Geology and petroleum potential of the Gulf of Mexico, Cuba. SPE Russian Oil and Gas Exploration and Production Technical Conference and Exhibition, Moscow, Russian; 14 – 16 October. SPE-171212-MS.
- [4]. Bryant, W. R., Lugo, J., Cordova, C., and Salvador, A., (1991). Physiography and bathymetry, in Salvador, A. ed., The Gulf of Mexico Basin, The Geology of North America, v. J. Geological Society of America, Boulder, CO, pp. 13–30.
- [5]. Ettensohn, F.R., (2008). The Appalachian foreland basin in the eastern United States, in Miall, A., ed., The Sedimentary basins of the United States and Canada: Sedimentary Basins of the World, Amsterdam, Elsevier, p. 105–179.
- [6]. Ewing, T.E., (1983). Growth faults and salt tectonics in the Houston diapir province: relative timing and exploration significance: Gulf Coast Association of Geological Societies Transactions, v. 33, pp 83–90.
- [7]. Ewing, T.E., (1991). Structural framework, in Salvador, A., ed., The Gulf of Mexico Basin: Boulder, Colo., Geological Society of America, The Geology of North America, v. J, p. 31–52.
- [8]. Miall, A. D., Catuneanu, O., Vakarelov, B., and Post, R., (2008). The Western Interior Basin, in Miall, A. D., (ed.), The Sedimentary Basins of the United States and Canada: Sedimentary basins of the World, vol. 5, K. J. Hsü, Series Editor, Elsevier Science, Amsterdam, pp. 329–362.
- [9]. Schlumberger, (2014). Petrel Advanced property modeling, training and exercise.
- [10]. Schlumberger, (2014). Petrel Fundamentals, Training and Exercise Guide.
- [11]. Schlumberger, (2015). Petrel Geology, training and exercise guide.
- [12]. Schlumberger, (2011). Petrel property modeling.
- [13]. Schlumberger, 2013. Petrel property modeling course.
- [14]. Steffens, G.S., Biegert, E.K., Sumner, H.S., and Bird, D., (2003). Quantitative bathymetric analyses of selected deep water siliclastic margins: receiving basin configurations for deep water fan systems. Marine and Petroleum Geology, v. 20, pp. 547–561.